



Numerical Study on the Effect of Installing Circular Cylinders in front of the Returning Blade and Beside the Advancing Blade of the Savonius Wind Turbine

Gusti Rusydi Furqon Syahrillah^{1,2}, Triyogi Yuwono^{1,*}, Vivien Suphandani Djanali¹

¹ Department of Mechanical Engineering, Faculty of Industrial Technology and Rekayasa System, Institut Teknologi Sepuluh Nopember, Keputih, 60111, Sukolilo Surabaya, Indonesia

² Department of Mechanical Engineering, Islamic University of Kalimantan, Jl. Adyaksa No. 2 Banjarmasin, Indonesia

ARTICLE INFO

Article history:

Received 6 March 2024

Received in revised form 19 May 2024

Accepted 15 June 2024

Available online 31 October 2024

Keywords:

Savonius wind turbine; circular cylinder; returning blade; advancing blade

ABSTRACT

Previous research has proven that placing a disruptive cylinder in front of the Savonius wind turbine's returning blade can significantly increase the performance of the Savonius turbine. In this study, two-dimensional unsteady simulations with a quadratic pave-type structured mesh showed that the circular cylinder placed in front of the returning blade and next to the advancing blade provides the best performance results at a free flow speed of 5 m/s and a Reynolds number of 100,000. In this study, the comparison with experimental data from another study is utilized. The Savonius turbine is installed with an interfering cylinder in front of the returning blade and next to the advancing blade; the air is tighter on the concave side of the advancing blade. The coefficient pressure difference between the convex and concave sides of the blade increases. The maximum moment is achieved in the turbine with a disturbance cylinder at a configuration distance of S/D 1.4 – Y/D 1.61. The maximum moment coefficient is obtained at the position $\theta = 15^\circ$. The placement of two cylinders with a ratio variation of 0.5 D can significantly influence turbine performance. Results show the turbine provides the highest Power Coefficient when $TSR = 0.6$. The power coefficient increased by 25.11% compared with that of conventional Savonius turbines. Therefore, it can be concluded that the turbine is the optimal configuration for generating the highest power.

1. Introduction

The decreasing availability of energy from fossil sources is beginning to affect human activity. To prevent climate change and protect the environment, the consumption of fossil fuels must be reduced. This can be accomplished in many ways, including substituting renewable energy sources for fossil fuels, such as solar, wind, tidal, and biomass, which are less harmful to the environment. To compensate for the dwindling supply of fossil fuels, alternative energy sources must be used. This is crucial to ensure that future generations can access these energy resources. We are responsible for

* Corresponding author.

E-mail address: triyogi@me.its.ac.id (Triyogi Yuwono)

<https://doi.org/10.37934/cfdl.17.4.1832>

ensuring the availability of alternative energy sources. Wind energy is one such alternative, with Savonius wind turbines exemplifying the use of wind as a renewable energy source.

The Savonius turbine operates on the principle of differing drag forces between the concave surface (advancing blade) and the convex surface (returning blade) of the turbine blades. This difference in drag creates a positive torque that spins the turbine and produces energy. The larger the disparity in drag forces, the more torque is generated.

Fluid movement within the turbine blade of a Savonius turbine generates positive and negative torques at the front and rear ends of the blade, respectively, which is a weakness. Additionally, the turbine's peak power output proportionally increases with increasing mass and size. This is caused by low turbine efficiency. As a result, many researchers have used numerical and experimental techniques to improve the performance of this type of wind turbine. The existing drawbacks of Savonius turbines include fluid flow over the turbine blades, which generates positive torque at the front and negative torque at the rear. In addition, the peak power output, which scales with increasing size and weight, contributes to the overall low efficiency. Due to the Savonius wind turbine's weakness, research is necessary for enhancing its performance (as shown in previous work [1-5]). Consequently, numerous researchers are conducting experiments and employing numerical methods to enhance the performance of this type of wind turbine. These deficiencies underscore the critical need for further investigation of Savonius Wind Turbines to improve their performance. Scholars interested in conducting investigations using numerical and/or experimental methods to improve the efficiency of Savonius turbines by adjusting the thickness, shape, or contour of the blades, as suggested by the authors of references from the previous study [6-8].

The authors have recommended that placing a circular cylinder on the upstream side of the returning blade at a distance of $S/D = 1.4$ results in the highest turbine power coefficient of about 12.2%, among the relative distances tested in their work. The method proposed by adding a circular cylinder around the Savonius turbine can be considered a passive control method, as mentioned in Triyogi *et al.*, [9].

This research is an effort made to improve the performance of this wind turbine by installing two circular cylinders simultaneously in front of the convex blade with a distance of $S/D = 1.4$ and next to the concave blade with a distance of $Y/D = 1.61$ and 2.00 . This circular cylinder directs airflow to the side of the concave blade so that the drag force on the blade side increases, thereby increasing the other torques. The diameter of the cylinder was fixed as described in a previous study Setiawan *et al.*, [10].

The stagger angles of a circular cylinder placed beside or upstream of a moving blade can vary, as shown in Refs. [11, 12]. Sakti *et al.*, [13] and Sanjaya *et al.*, [14] positioned a circular cylinder with both sides at a 65° angle, on the upstream side in front of the returning blade. The Savonius turbine's performance has been improved through modified turbine configurations in these studies. Guo *et al.*, [15] experimentally added a circular cylinder to the upstream side of the returning blade for additional enhancements.

The research gap addressed in this study is that previous studies have only employed a single variation of circular cylinder placement, either in front of the returning blade or beside the advancing blade. In contrast, this study combines both aspects with the aim of enhancing the performance of the Savonius turbine. This research is particularly compelling because no previous studies have combined these two methods, making it essential to investigate the resulting flow phenomena and their impact on turbine performance.

2. Methodology

Three simulations were conducted, involving configuration A where a cylinder was installed ahead of the returning (S/D) blade with a ratio of 1.4, similar to studies by Francis *et al.*, [7] and Triyogi *et al.*, [8], and configuration B featuring a circular cylinder attached next to the advancing blade at designated distances of 1.42, 1.51, 1.61, 1.71, and 1.82. By combining configurations A and B, configuration C is obtained with the specified S/D and Y/D values (S/D 1.4 - Y/D 1.42, 1.51, 1.61, 1.71, 1.82), as shown in Figure 1 :

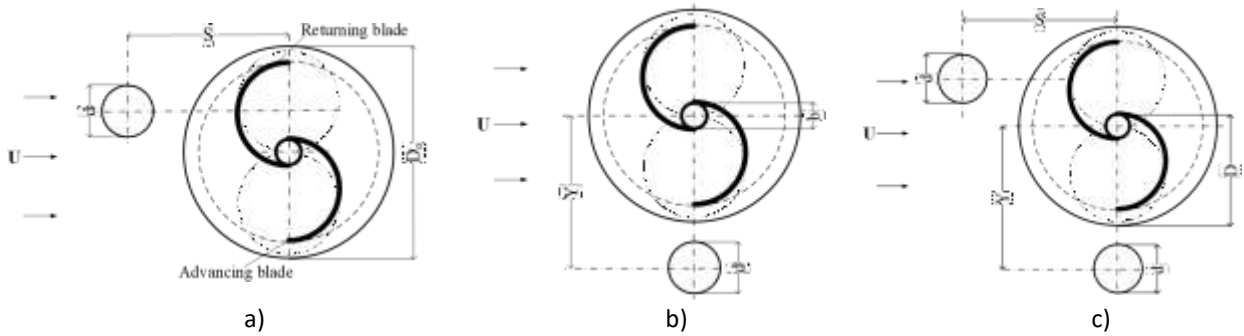


Fig. 1. Savonius turbine and circular cylinders in configurations: (a) configuration-A, (b) configuration-B, and (c) configuration-C

The ratio of the circular cylinder diameter to the rotor diameter (d/D) is 0.5, the distance relative to the rotor diameter (S/D) was kept constant at 1.4, and the distance between cylinder center and turbine center (Y/D) is 1.42, 1.51, 1.61, 1.71 and 1.82 as shown in Figure 2. Reynolds number exceeds 100,000. This design is intended to improve the Savonius turbine performance in terms of the power coefficient (C_p), moment coefficient (C_m), and static torque (CTS). In this study, the simulation followed the experimental conditions described in previous study by Sanjaya *et al.*, [14] also Lee *et al.*, [17].

The ANSYS/Fluent 2021.1 software was used to perform numerical simulations of this study. Two domains comprise the Savonius turbine geometry: the static and rotating domains. A static domain is not in motion and is traversed by a fluid. The rotating domain rotates through the fluid.

Figure 2 and Figure 3 depict the computational domain of the proposed turbine. In Figure 3, the domain is the detailed domain around the turbine. The size is 750 cm by 300 cm. The rotating turbine region and the stationary disturbing cylinder region constitute the domain, which is divided by an interface. To simplify the numerical simulations, the domain was divided into static and rotating parts. The domain's division streamlines meshing and solver setup processes.

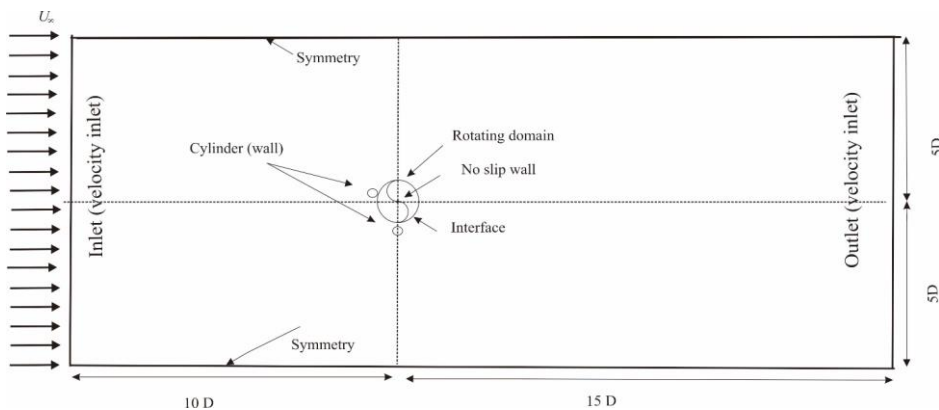


Fig. 2. Computational domain

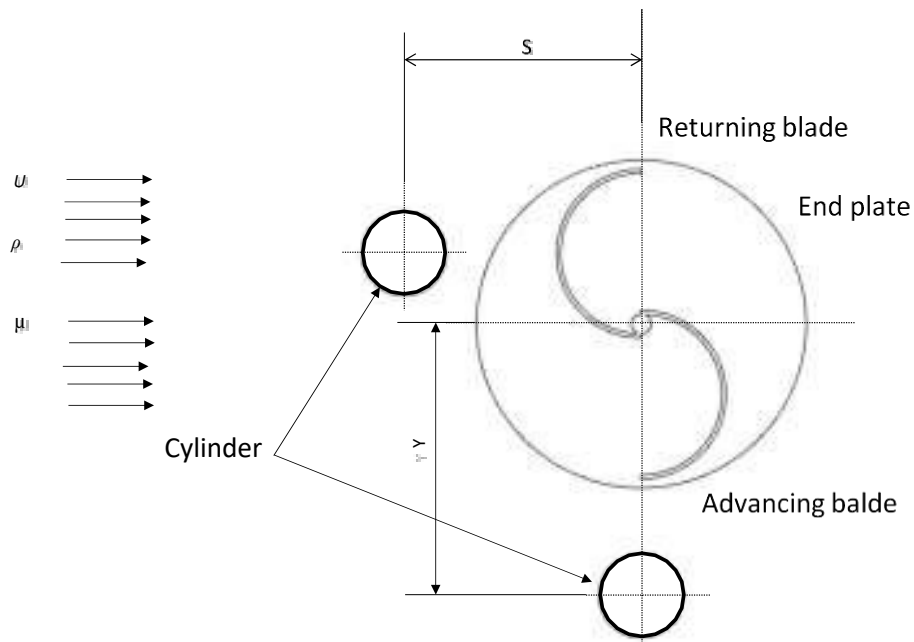


Fig. 3. Detailed view around Savonius blade

In simulations, meshes or grids are formed based on the interpretation of volumes or the spatial domain over which calculations are performed. Choosing an appropriate mesh size enhances the accuracy of a CFD simulation. Reducing the mesh size enhances the model's result precision. Though a finer mesh yields greater accuracy, it demands more computational power and time. Properly modifying the mesh size, using smooth meshing, is crucial to obtaining accurate results while conserving computational resources. The 2D simulation includes a Savonius turbine with a quadratic mesh structure, as shown in Figure 4. Figure 5 shows an enlarged version. In this modeling, mesh selection is performed for validation to obtain accurate results close to those of previous studies.

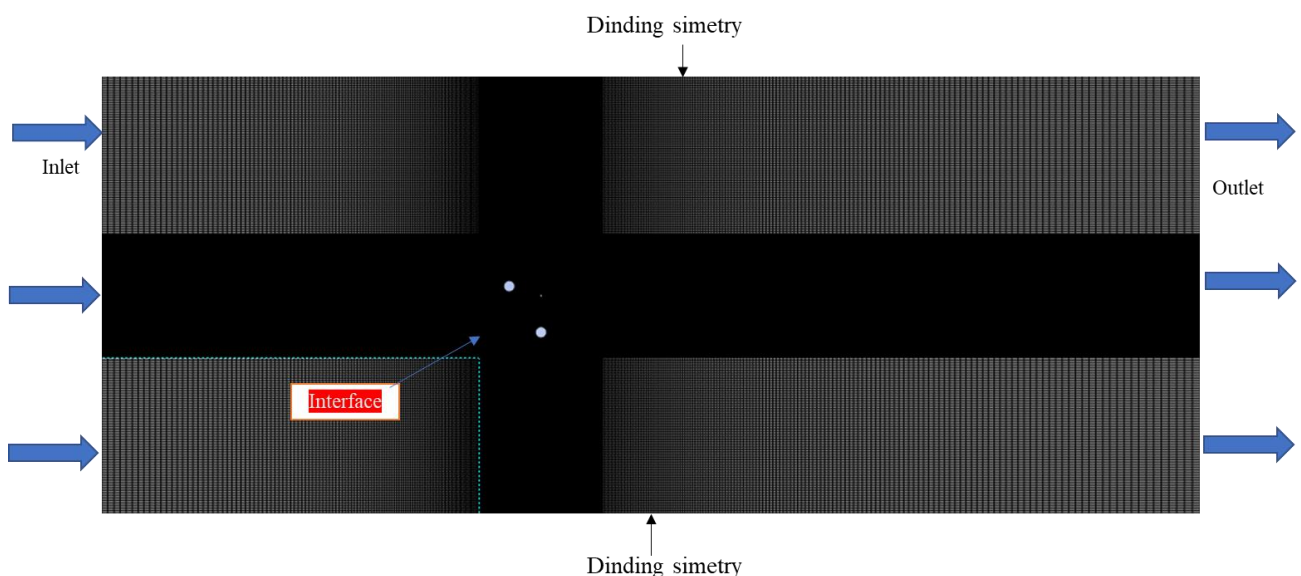


Fig. 4. Computational grid

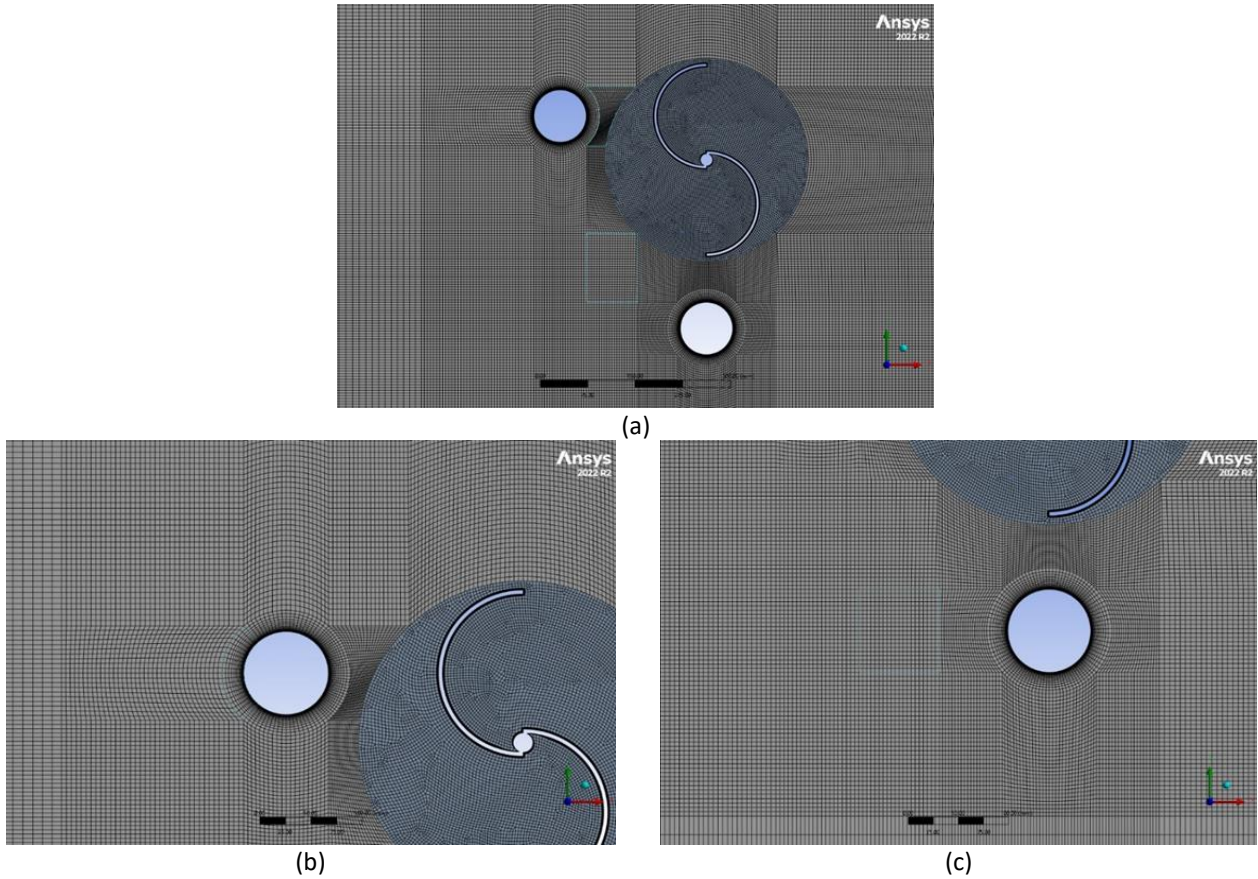


Fig. 5. (a, b, c) Fixed zone and Rotating zone area enlarged with Meshing structured with Quadratic Pave type

2.1 Processing

The Reynolds number (Re) can be determined by Eq. (1).

$$Re = \frac{\rho V D}{\mu} \quad (1)$$

Where Re is the Reynold number, ρ is the density of water, μ is the Dynamic viscosity of water, and D is the hydraulic diameter.

According to [16], the time step was calculated for each degree of increase in the turbine rotation angle. The maximum number of iterations for every step up to 50 indicates convergence within 50 iterations for 10 turbine rotations. The convergence criterion is set when the continuity and other residual parameters reach below 10^5 . The time step size (TSS) was calculated using Eq. (2) as follows:

$$TSS = T_{rot} \frac{\theta}{360} = \frac{\theta}{(6 \times N)} \quad (2)$$

Where θ is the increment angle or degree of rotation of the time step, and N is the turbine rotation; thus, T_{rot} is the time of one rotation, which can be determined by Eq. (3):

$$I_{rot} = \frac{60}{N} \quad (3)$$

Considering to measurement of rotational speed (ω) and the free stream velocity (U), the tip speedratio (λ) can then be defined as in Eq. (4):

$$\lambda = \frac{\omega L}{2U} \quad (4)$$

Based on the dynamic torque measured (T_d), the moment coefficient can be calculated as in Eq. (5):

$$Cm = \frac{4T_d}{\rho U^2 H L^2} \quad (5)$$

Where H is the height of the turbine blade, and the power coefficient (C_p) is defined as in Eq. (6):

$$Cp = \frac{2T_d \omega}{\rho U^3 H L} = Cm \lambda \quad (6)$$

A comprehensive overview set up of the simulation shown in Table 1 below:

Parameter	Input
General Solver	Pressure based, transient, 2D
Model Viscous	Realizable k ϵ (RKE)
Material Air	$\rho = 1,184 \text{ kg/m}^3$: $\mu = 1,789 \cdot 10^{-5} \text{ kg/m.s}$
Cell zone condition Rotating/ Fixed domain	Mesh motion, Rotating velocity, Material air
Boundary condition Inlet	Velocity 5 m/s Spec. method Intensity and length scale Turbulence Intensity 3.78 % Turbulence length scale = 2.24
Wall Savonius Cylinder	Moving - Wall Rotational - No slip Stationary wall - No slip
Mesh interface	Interface1, interface2
Reference Value Compute from Area Length	Inlet 0.090 m ³ 0.500 m
Solution methods Pressure Gradient Momentum Turbulence Kinetic Energy Residual	Simple Least Squares cell-based Second order Second order Second order Absolute criteria 10 ⁻⁵
Run Calculation	Number of time steps = 3600 Max iteration /Time step 50
Time Step Size	Calculated according to the $T_{SR} = 0.6$

In this study, the simulation was performed using the commercial fluid flow solver ANSYS. The Semi-Implicit Method for Pressure-Linked Equation (SIMPLE) and the turbulence model realizable k-

e with enhanced wall treatment are used to solve the equation of Unsteady Reynolds Average Navier–Stokes (URANS) was used. The Sliding Mesh Model (SMM) was used to discretize all variables and turbulence intensity discretely within the finite volume formulation in the second-order upwind scheme and unsteady flow. The data acquired during the preceding phase were examined and interpreted. The provided data consist of the speed and pressure contours, moment, and power, which are measured on both the advancing and returning blades. These measurements are presented as functions of the angle (θ).

The grid independence test is a crucial step in the process of generating a mesh with varying numbers of cells. The purpose of this study is to identify the most suitable grid configuration that yields the correct results using a configuration as a reference. The simulation data are compared with the reference configuration to obtain results that are quantified as a percentage error. Figure 6 below presents the outcomes of the grid independence examination conducted on the Savonius wind turbine in Figure 6 below:

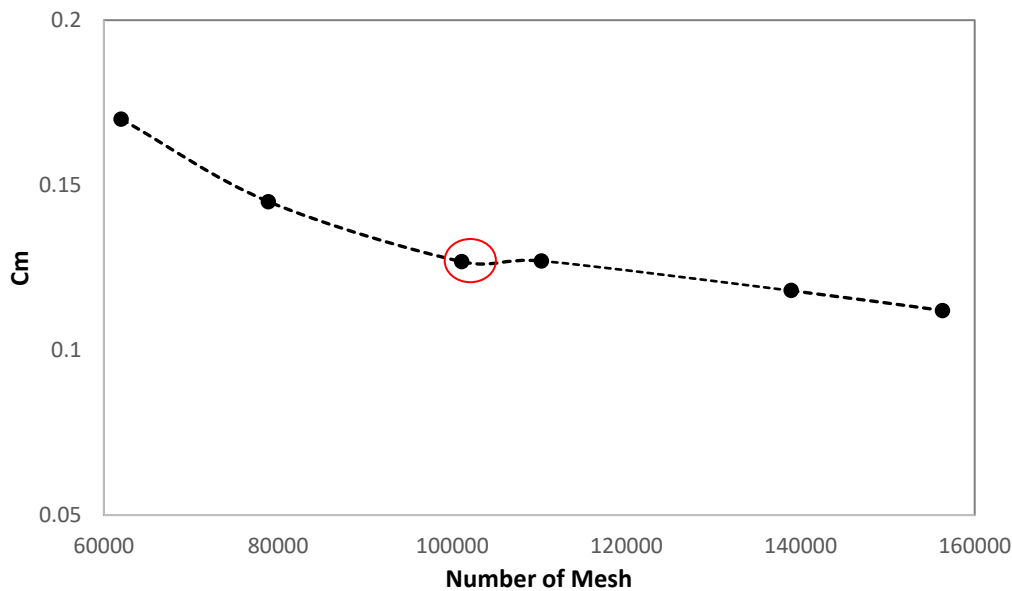


Fig. 6. Computational grid graph

In the simulation, a 101108-element mesh was employed. A mesh with a stable average coefficient of moment value, as the number of element increases, was selected. The small error value further demonstrates this. Considering the longer simulation time required for a finer mesh, we opted for a mesh containing 101108 elements, as shown in Figure 6.

Figure 7 presents a validation graph that compares the results obtained from both experimental and simulation studies. The graph exhibits a similar trend, specifically, a decline in the coefficient of moments as TSR increases. The discrepancies in the obtained values were minimal (5%). Because of the significant similarity between the simulation and experimental results, we conclude that the simulation outcomes are accurate.

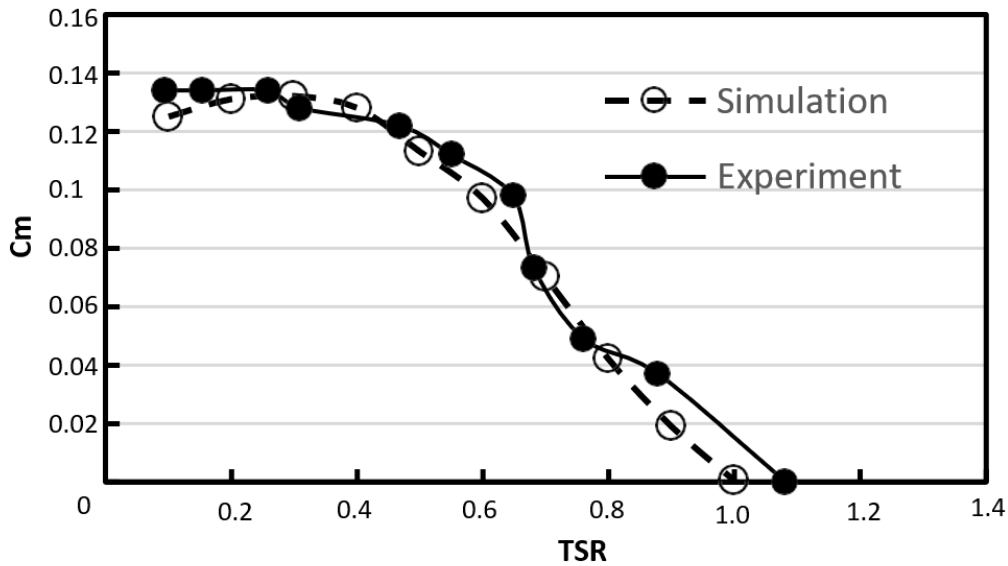


Fig. 7. Graph of C_m versus T_{SR} for a conventional turbine at low speed, 5 m/s

3. Results

The study's results include both quantitative data (C_m values) and qualitative data (velocity contours), allowing comparison of the Savonius turbine configuration with and without the addition of a cylinder using their respective C_m graphs and azimuth angles (as shown in Figure 8). At azimuth angles of 30° , 60° , 90° , and 150° , Figure 8 illustrates noticeable differences in C_m between the two configurations. A cylindrical configuration at a 30° angle yields up to 70% more height than a traditional turbine. At an azimuth angle of 60° , the conventional turbine experiences a larger C_m of up to 70% compared to other angles. For an azimuth angle of 90° , the disparity in C_m between cylindrical and conventional configurations decreases as the difference in C_m for the conventional configuration decreases to 30%. For an azimuth angle of 150° , the cylinder configuration in the new design is 50% more effective than that in the traditional design.

Velocity contours are required for a thorough understanding of the physical reasons behind the difference in C_m due to different cylinder configurations. Figure 9, Figure 10, Figure 11, and Figure 12 demonstrate the flow pattern through turbines at various angles, specifically 30° , 60° , 90° , and 150° , revealing the impact of the disturbing cylinder on the S/D 1.4 – Y/D 1.6 setup. The analysis zeroes in on angles where C_m 's difference is substantial.

Configuration C of the Savonius Turbine in Figure 9 operates more efficiently at an angle of 30° than both A and B. The cylinder addition at Y/D 1.6 shown in figure 9 enhances the flow velocity adjacent to the convex side of the advancing blade compared to configurations A and B. The flow narrows significantly as the cylinder approaches the turbine corner, resulting in a nozzle-like flow condition. The increase in turbine speed reduces the pressure in the opposite direction, thereby increasing C_m . At an azimuth angle of 60° (Figure 8), the conventional configuration's C_m is greater than S/D's 1.4-Y/D1.6. At an azimuth angle of 60° , the S/D 1.4 cylinder's speed is slower than that of the conventional configuration. The wake from the cylinder causes both a decrease in speed and an increase in pressure. The increase in pressure reduces the Savonius tube blade's returning force in the direction opposite to its rotation. In a conventional turbine, C_m is greater than that with the inclusion of an extra cylinder.

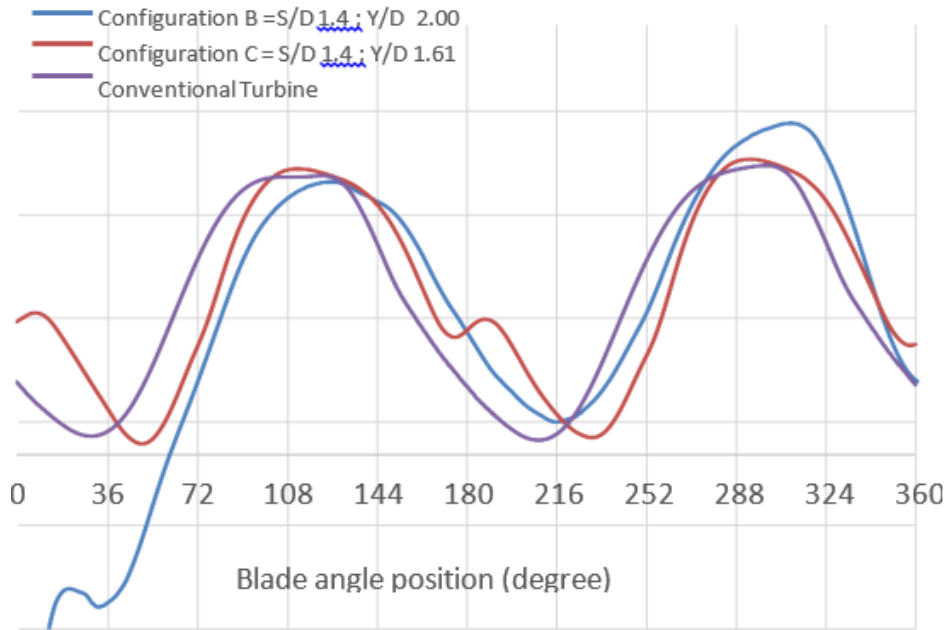


Fig. 8. The evolution of the coefficient of moment corresponds to the angle of increment of the turbine blade and the ratio between the two variables

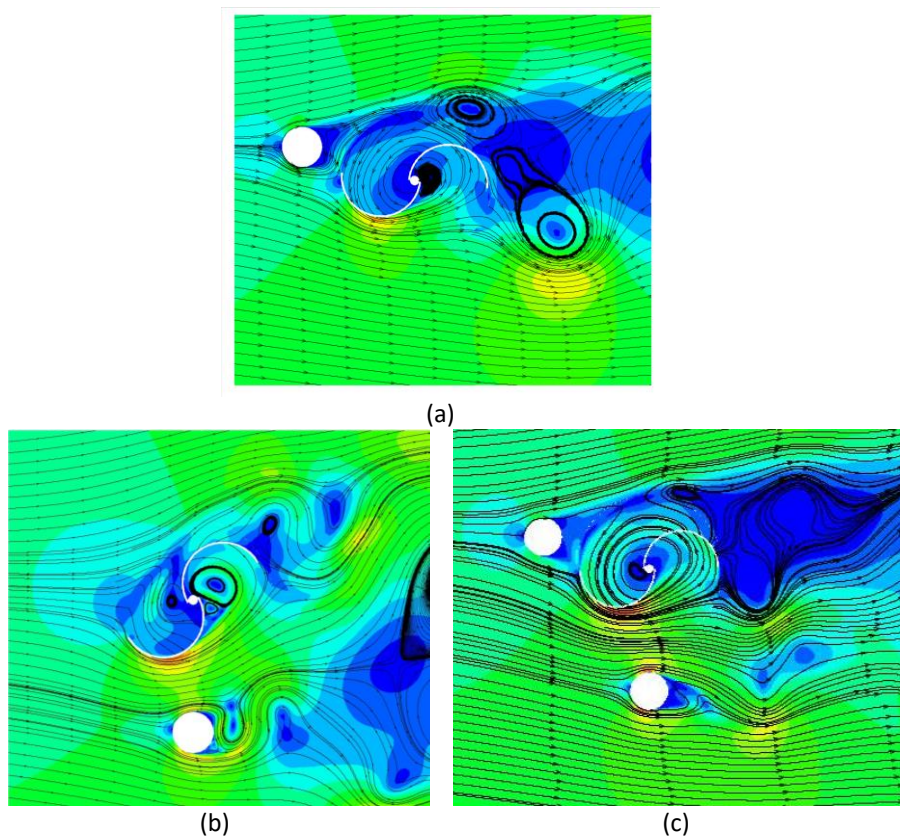


Fig. 9. Comparison of speed profiles turbine 30° at a speed of 5 m/s in (a) configuration A, (b) configuration B, and (c) configuration C

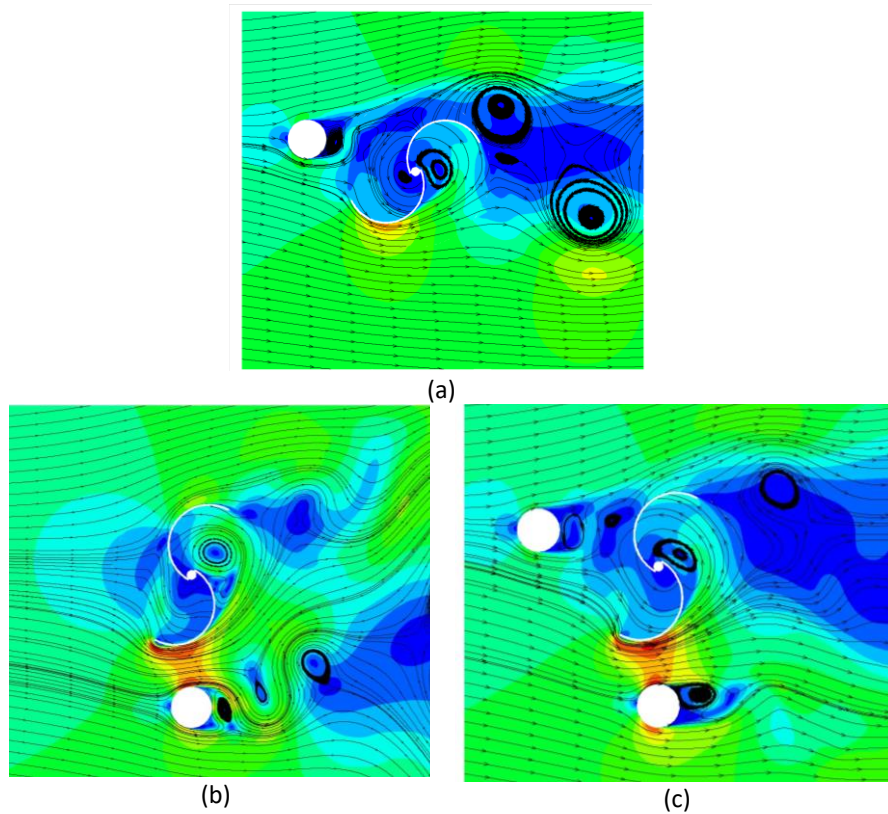


Fig. 10. Comparison of speed profiles turbine 60° at a speed of 5 m/s in (a) configuration A, (b) configuration B, and (c) configuration C

For Figure 11 at an azimuth angle of 90°, the phenomenon that occurs is not much different from that when the Savonius Turbine is at an azimuth angle of 60°, where the pressure on the blade returning cylindrical configuration is greater than that of the conventional configuration due to increased pressure from the wake cylinder. However, the difference in the C_m values decreases. Decrease in the difference in C_m values, when viewed from Figure 10 (contour image), is due to the increase in speed from the nozzle effect provided by the Y/D 1.6 cylinder so that the pressure on the convex side of the advancing blade decreases, reducing the pressure in the opposite direction of the turbine rotation. The C_m of the cylindrical configuration is larger than that of the conventional configuration at an azimuth angle of 150° (Figure 12). In the figure (contour image), vortex flow forms around the central corner of the turbine. Vortex flow is formed by concurrent flow along the horizontal axis and the flow following turbine rotation, predominantly near the axis. Because of the differing flow directions toward the turbine blade's rotation and horizontal axis, vortex forms in the flow. The Savonius turbine's performance is hindered by the high-pressure vortex flow. At S/D 1.4, the cylinder generates a wake that obscures the flow in the horizontal direction. The absence of horizontal flow hinders the formation of a vortex and reduces the force output of the Savonius turbine.

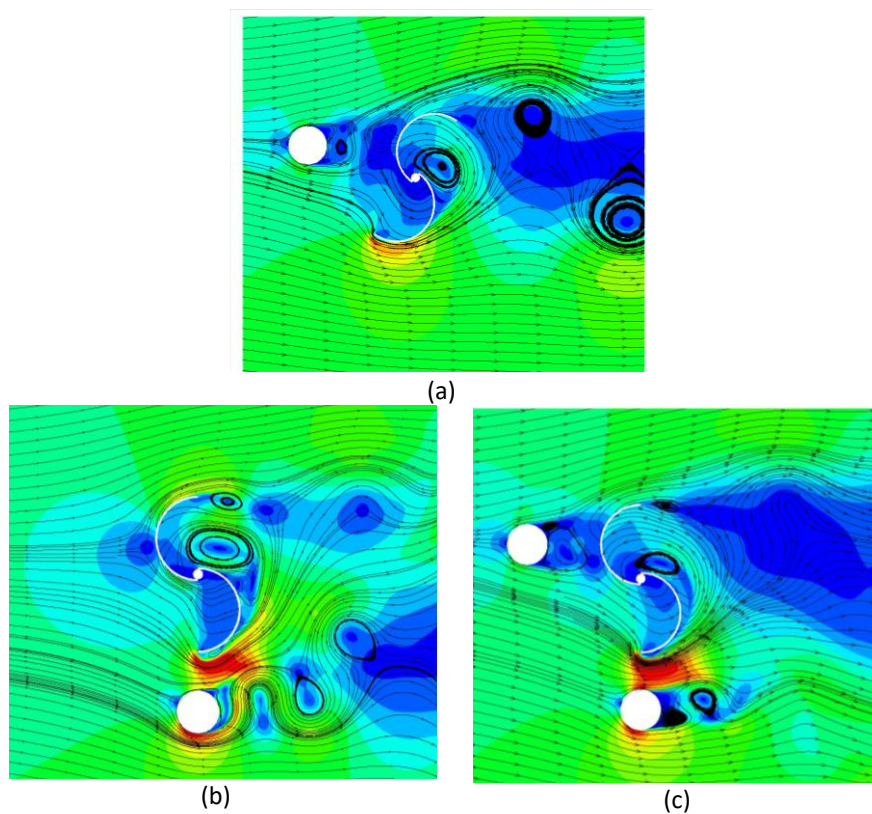


Fig. 11. Comparison of speed profiles turbine 90° at a speed of 5 m/s in (a) configuration A, (b) configuration B, and (c) configuration C

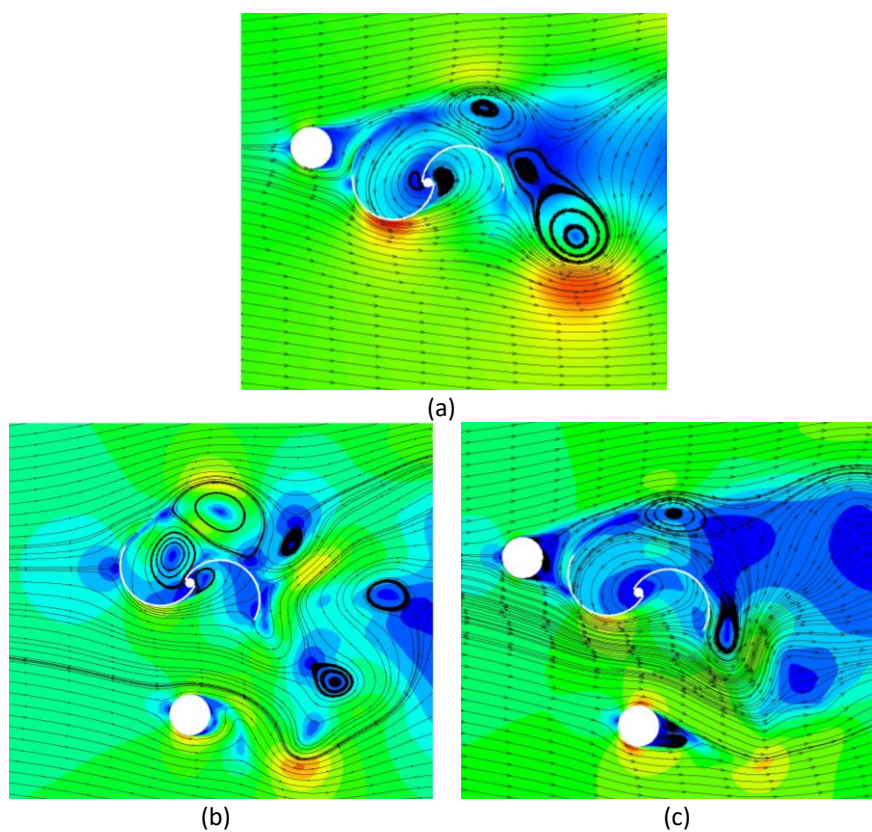


Fig. 12. Comparison of speed profiles turbine 150° at a speed of 5 m/s in (a) configuration A, (b) configuration B, and (c) configuration C

The comparison graph (Figure 13) displays the coefficient of power (CoP) values for a conventional turbine with configurations S/D 1.4 – Y/D 1.61 and 1.4 – Y/D 1.82 at a wind speed of 5 m/s, plotted against their respective tip speed ratios (λ). The addition of cylinders in front of the retracting blade and next to the advancing blade in a Savonius wind turbine (Y/D configuration) enhances its performance compared with conventional designs. The power coefficient has significantly increased, resulting in enhanced performance. A cylinder with a configuration of S/D 1.4 – Y/D 1.61 = 1.51 yielded the greatest CoP value (0.068) for the Savonius wind turbine when the TSR was 0.6.

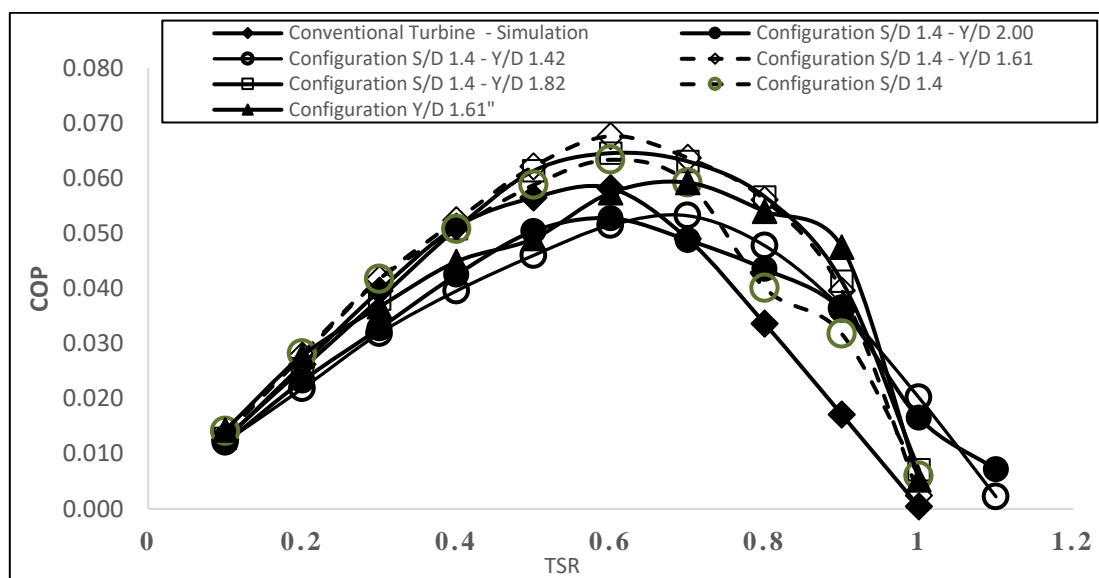


Fig. 13. Graph of Coefficient Power (CoP) versus Tip Speed Ratio (λ) of conventional turbines and various distance configurations simulation at wind speed 5 m/s

The Savonius wind turbine's TSR function coefficient is displayed in Figure 14 with the cylinder placements: one next to the advancing blade and the other in front of the returning blade for the second configuration. Among the turbine variations shown on the graph, the one featuring a cylinder in front of the returning blade and next to the advancing blade has the highest S/D ratio (1.4) and Y/D ratio (1.61). The middle TSR value results in the best turbine performance. Each turbine's TSR should be set for maximum power production. At a TSR of 25.11%, a turbine with a cylinder shows an increase in value of approximately 61% compared to one without a cylinder when the S/D ratio is 1.4. The cm value was nearly diminished in other TSRs. For variable S/D 1.4, the Cm value increases by 13.34% when Y/D is 1.82. Adding a cylinder in front of the returning blade decreases the pressure on its convex side. The cylinder distance influences the air flow and shear layer up to the turbine, subsequently boosting the Cm value.

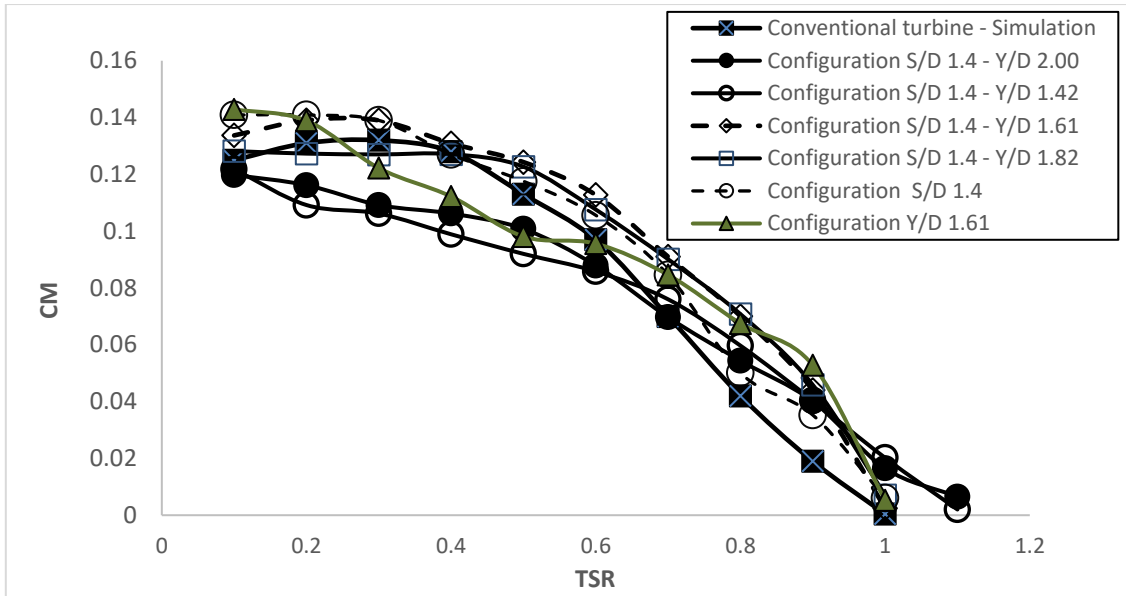


Fig. 14. Graph of Coefficient of the moment (Cm) against Tip Speed Ratio (TSR) of conventional turbines, Configuration S/D 1.4 – Y/D 1.61 and S/D 1.4 – Y/D 1.82, simulated at a wind speed of 5 m/s

Figure 15 depicts the Coefficient of Pressure (CoP) for both conventional and cylindrical configurations, with S/D ratios between 1.4 and 1.6 and a 30° angle. The azimuth angle of 300° was selected because the difference in effective capacitance between the traditional and cylindrical geometries exceeded 70%. The difference in CoP is notably large near the center of the turbine in Figure 8, occurring only when X/L exceeds 0.1. A lower CoP signifies a quicker blade speed in the reverse configuration than in the conventional configuration. The addition of a cylinder triggers turbulent flow, thereby providing more blade momentum and reduced pressure.

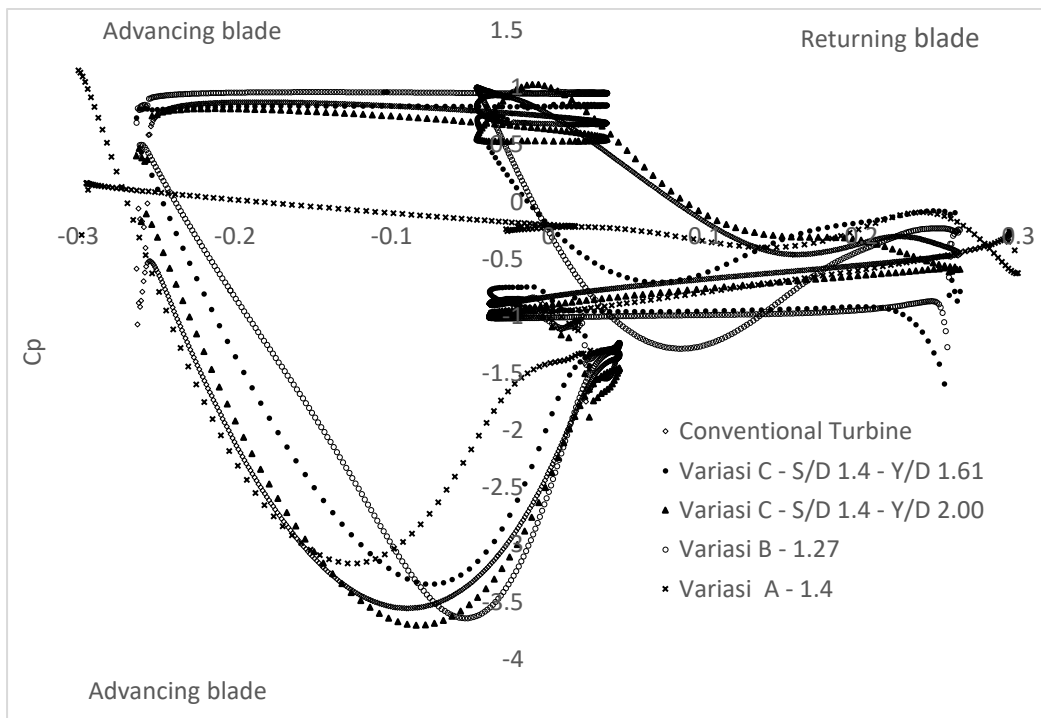


Fig 15. Distribution of Coefficient pressure along the surface of the Savonius turbine blade at Tip Speed Ratio $\lambda = 0.6$ with an angle of 30°

The conventional turbine exhibits a smaller drop in CoP compared to the cylindrical configuration, suggesting a less pronounced speed increase. The smaller cylindrical configuration's CoP area on the returning blade results in reduced drag force. At an azimuth angle of 30°, adding a cylinder increases flow momentum and thereby reduces drag force on the returning blade, leading to pressure reduction. In conventional turbines, the CoP area is larger on the advancing blade than in cylinders. Flow velocity decreases in the Y/D 1.6 cylinder due to stagnation pressure at the advancing blade. The stagnation pressure reduction behind the blade results in a decrease in flow through it. The reduced flow on the advancing blade increases the pressure. The advantage of cylindrical shaping on the returning blade side outweighs the slowdown effect due to stagnation pressure on the advancing side, resulting in a potential increase in drag coefficient of up to 70%.

4. Conclusions

Based on the simulation results, a conclusion can be drawn below:

- i. Installing a circular cylinder 1.4 m away from the Savonius wind turbine return blade enhances turbine performance by 19% more efficiency in the return blade area, resulting in decreased pressure.
- ii. Among configurations B, the turbine performance can be enhanced notably at Y/D = 1.42 and 1.61. The maximum CoP improvement of over 25% occurs at Y/D = 1.61, TSR = 0.69.
- iii. At a TSR of 0.6, the Cm value rises by 0.16 when S/D equals 1.4 and Y/D equals 1.61. The addition of a cylinder in front of the returning blade and next to the advancing blade at varying distances S/D = 1.4 and Y/D = 1.61 results in higher moment values (Cm) at an azimuth of 30° than without a cylinder. The performance boost was 25.11% more efficient than conventional turbines.

Acknowledgement

This study is funded by the Doctoral Dissertation Research Program (Grant No. 112/E5/PG.02.00.PL/2023) of the Ministry of Education, Culture, Research, and Technology of the Republic of Indonesia.

References

- [1] Altan, Burçin Deda, and Mehmet Atılğan. "The use of a curtain design to increase the performance level of a Savonius wind rotors." *Renewable Energy* 35, no. 4 (2010): 821-829. <https://doi.org/10.1016/j.renene.2009.08.025>
- [2] Mao, Zhaoyong, and Wenlong Tian. "Effect of the blade arc angle on the performance of a Savonius wind turbine." *Advances in Mechanical Engineering* 7, no. 5 (2015): 1687814015584247. <https://doi.org/10.1177/1687814015584247>.
- [3] G Sakti, T. Yuwono. "Numerical And Experimental Investigation of The Effect of a Circular Cylinder as Passive Control on The Savonius Wind Turbine Performance." *Journal of Southwest Jiaotong University* 56, no. 6 (2021). <https://doi.org/10.35741/issn.0258-2724.56.6.7>
- [4] Yuwono, Triyogi, Gunawan Sakti, Fatowil Nur Aulia, and Adi Chandra Wijaya. "Improving the performance of Savonius wind turbine by installation of a circular cylinder upstream of returning turbine blade." *Alexandria Engineering Journal* 59, no. 6 (2020): 4923-4932. <https://doi.org/10.1016/j.aej.2020.09.009>.
- [5] Putri, Nabila Prastiya, Triyogi Yuwono, Jasmi Rustam, Prayogi Purwanto, and Galih Bangsa. "Experimental studies on the effect of obstacle upstream of a Savonius wind turbine." *SN Applied Sciences* 1 (2019): 1-7. <https://doi.org/10.1007/s42452-019-1253-2>.
- [6] Lee, Sang-Joon, Sang-Ik Lee, and Cheol-Woo Park. "Reducing the drag on a circular cylinder by upstream installation of a small control rod." *Fluid dynamics research* 34, no. 4 (2004): 233. <https://doi.org/10.1016/j.fluiddyn.2004.01.001>

- [7] Francis M. Vanek, Louis D. Albright 2008. *Energi Systems Engineering*, Mc. Graw Hill, Newyork.
- [8] Yuwono, Triyogi, Abdul Latip, Nabila Prastiya Putri, Mukhamad Ubaidillah, Erik Noer Mazhilna, Citro Ariyanto, Ulfah Andaryani, Anas Fauzi, Wawan Aries Widodo, and Bambang Arip Dwiyantoro. "The effect of width of single curtain on the performance of Savonius wind turbine." In *AIP conference proceedings*, vol. 1983, no. 1. AIP Publishing, 2018. <https://doi.org/10.1063/1.5046219>
- [9] Triyogi, Y., D. Suprayogi, and E. Spirda. "Reducing the drag on a circular cylinder by upstream installation of an I-type bluff body as passive control." *Proceedings of the Institution of Mechanical Engineers, Part C: Journal of Mechanical Engineering Science* 223, no. 10 (2009): 2291-2296. <https://doi.org/10.1243/09544062JMES1543>
- [10] Setiawan, Priyo Agus, Triyogi Yuwono, Wawan Aries Widodo, Eko Julianto, and Mardi Santoso. "Numerical study of a circular cylinder effect on the vertical axis Savonius water turbine performance at the side of the advancing blade with horizontal distance variations." *International Journal of Renewable Energy Research* 9, no. 2 (2019): 978-985.
- [11] Sakti, Gunawan, Triyogi Yuwono, and Wawan Aries Widodo. "Experimental and Numerical Investigation of I-65° Type Cylinder Effect on the Savonius Wind Turbine Performance." In *International Journal of IOP Conf. Series: Earth and Environmental Science*, vol. 505, p. 012042. 2020.
- [12] Setiawan, Priyo Agus, Triyogi Yuwono, and Wawan Aries Widodo. "Effect of a circular cylinder in front of advancing blade on the Savonius water turbine by using transient simulation." *International Journal of Mechanical and Mechatronics* 19, no. 01 (2019): 151-159.
- [13] G Sakti, T. Yuwono. "Numerical And Experimental Investigation of The Effect of a Circular Cylinder as Passive Control On The Savonius Wind Turbine Performance." *Journal of Southwest Jiaotong University* 56, no. 6 (2021). <https://doi.org/10.35741/issn.0258-2724.56.6.7>
- [14] Sewucipto, Sanjaya, and Triyogi Yuwono. "The influence of upstream installation of D-53° type cylinder on the performance of Savonius turbine." *Journal of Advanced Research in Experimental Fluid Mechanics and Heat Transfer* 3, no. 1 (2021): 36-47.
- [15] Guo, Fen, Baowei Song, Zhaoyong Mao, and Wenlong Tian. "Experimental and numerical validation of the influence on Savonius turbine caused by rear deflector." *Energy* 196 (2020): 117132. <https://doi.org/10.1016/j.energy.2020.117132>
- [16] Mohamed, M. H., G. Janiga, E. Pap, and D. Thévenin. "Optimization of Savonius turbines using an obstacle shielding the returning blade." *Renewable Energy* 35, no. 11 (2010): 2618-2626. <https://doi.org/10.1016/j.renene.2010.04.007>
- [17] Lee, Jae-Hoon, Young-Tae Lee, and Hee-Chang Lim. "Effect of twist angle on the performance of Savonius wind turbine." *Renewable Energy* 89 (2016): 231-244. <https://doi.org/10.1016/j.renene.2015.12.012>